# Correlated cortical populations can enhance sound localization performance

Rick L. Jenison[a)]
*Department of Psychology, University of Wisconsin, Madison, Wisconsin 53706*

(Received 8 March 1999; revised 16 July 1999; accepted 20 September 1999)

Neurons within cortical populations often evidence some degree of response correlation. Correlation has generally been regarded as detrimental to the decoding performance of a theoretical vector-averaging observer making inferences about the physical world—for example, an observer estimating the location of a sound source. However, if an alternative decoder is considered, in this case a Maximum Likelihood estimator, performance can improve when responses in the population are correlated. Improvement in sound localization performance is demonstrated analytically using Fisher information, and is also shown using Monte Carlo simulations based on recordings from single neurons in cat primary auditory cortex. © *2000 Acoustical Society of America.* [S0001-4966(00)01501-0]

PACS numbers: 43.64.Bt, 43.64.Qh [RDF]

## INTRODUCTION

Statistical independence of cortical responses is often assumed for the theoretical study of neural coding. Under the assumption of independence, simple population averaging of even weakly correlated sensory neurons can result in diminished performance compared to a neural population composed of independent neurons (Zohary *et al.*, 1994; Shadlen *et al.*, 1996; Shadlen and Newsome, 1998). However, it can be shown that a Maximum Likelihood (ML) estimator with knowledge of the population response covariance matrix can demonstrate improvement in estimation performance when the responses within a population are correlated. This perhaps surprising result can be demonstrated both analytically using Fisher information, and confirmed using Monte Carlo simulation. Much has been written on the topic of estimation theory, the roots of which extend back to Ronald Fisher (1925). Estimation theory is concerned with the problem of finding a best value for an unknown parameter from a measured sample. We, as well as others, have previously investigated the consequences of broad receptive fields on population coding using Fisher information and the Cramer–Rao lower bound (CRLB) under the assumption of independence (Paradiso, 1988; Seung and Sompolinsky, 1993; Jenison, 1998). More recently Abbott and Dayan (1999) have shown that, in theory, correlation can have a positive impact on the acuity of a population code using the analytic tools of Fisher information and the CRLB. However, their analysis was restricted to the coding of a single parameter, hence they did not consider the impact of correlation on cross-information between parameters such as sound source localization in two dimensions, i.e., azimuth and elevation.

The CRLB is a lower bound on the variance of any unbiased estimator, and is derived from Fisher information with respect to a family of parametric probability distributions. The CRLB is inversely related to Fisher information mathematically, and intuitively. As the magnitude of Fisher information increases, we expect estimation error variance to diminish. In addition, it can be shown that ML estimation performance asymptotically approaches the CRLB as the number of measurements becomes large (Blahut, 1987). If the CRLB can be derived analytically, it can be used to compute the minimum possible variance about any value estimated by a theoretical ideal observer. The power of this analysis is the following: whatever form of biological information processing ensues on the population of cortical responses, the very best performance, defined in terms of estimation variability, is given by the CRLB. This lower bound applies to the brain, as well as any other decoding mechanism. Under the assumption of independence, even very broad and nonuniform spatial receptive fields in primary auditory AI cortex can demonstrate psychophysical localization acuity with as few as ten cells in the population (Jenison, 1998). Although it is quite unlikely that this optimal form of estimation is literally performed by cortical circuitry, some recent modeling work has shown that simple recurrent neural networks can be used to approximate the mechanics of ML estimation (Pouget *et al.*, 1998). ML estimation provides an upper bound on performance given empirically measured responses and affords one way of assessing the relative magnitude of information available at different levels along a sensory pathway.

## I. MODELS

We have recently described a methodology by which cortical receptive fields that depend on the location (azimuth $\theta$ and elevation $\phi$) of a virtual sound source in space can be functionally modeled (Jenison *et al.*, 1998). The methods used to collect the single neuron responses that constrain the receptive field models are described in Brugge *et al.* (1996), which are briefly summarized here. Barbiturate-anesthetized cats were fitted with hollow ear pieces sealed into the external ear canals through which virtual acoustic space stimuli (Musicant *et al.*, 1990) were presented. Single neurons were recorded extracellularly in the high-frequency region of the left AI field of auditory cortex. The latency of the first-spike

[a)]Electronic mail: jenison@wavelet.psych.wisc.edu

in response to transient virtual acoustic space stimuli was used as the primary response variable for von Mises basis function approximation[1] (Jenison *et al.*, 1998). Although we have found these basis functions to yield accurate models of spatial receptive fields, the analysis described here does not depend on any specific receptive field model. Hence the $i$th modeled spatial receptive field in a cortical population will be denoted *symbolically* as $\widehat{\mathbf{SRF}}_i(\theta,\phi)$. The derivative operators applied to the receptive fields, i.e., $(\partial/\partial\theta)\widehat{\mathbf{SRF}}_i(\theta,\phi)$ and $(\partial/\partial\phi)\widehat{\mathbf{SRF}}_i(\theta,\phi)$, denote the receptive field gradient or slope relative to a change in azimuth or elevation. The ''hat'' ($\hat{}$) implies a mathematical model that approximates the behavior of a set of actual measurements.[2]

In this study, performance is measured in terms of estimation variability of a chosen target direction resulting from a sample of population responses. The structure of the noise covariance between neurons, under a simplifying assumption of homogeneous correlation[3] within the population, can be formally characterized as

$$\mathbf{G}_{\text{resp}}=\begin{bmatrix} \sigma_1^2 & \rho_{\text{resp}}\sigma_1\sigma_2 & \cdots & \rho_{\text{resp}}\sigma_1\sigma_N \\ \rho_{\text{resp}}\sigma_2\sigma_1 & \sigma_2^2 & \vdots & \rho_{\text{resp}}\sigma_2\sigma_N \\ \vdots & \cdots & \ddots & \vdots \\ \rho_{\text{resp}}\sigma_N\sigma_1 & \rho_{\text{resp}}\sigma_N\sigma_2 & \cdots & \sigma_N^2 \end{bmatrix}, \quad (1)$$

where $\sigma_i^2$ is the variance of the noise about the $i$th modeled receptive field and $\rho_{\text{resp}}$ is the response correlation coefficient. The off-diagonal cells correspond to covariance between the $i$th and $j$th neurons. Given this covariance structure, the probability density function of the population response array, denoted $\overrightarrow{\text{resp}}$, given a particular location in space ($\theta$, $\phi$) under a Gaussian assumption is

$$p(\overrightarrow{\text{resp}}\,|\,\theta,\phi)=\frac{1}{\sqrt{(2\pi)^N|\mathbf{G}_{\text{resp}}|}} \times\exp\left(-\tfrac{1}{2}(\overrightarrow{\text{resp}}-\widehat{\mathbf{SRF}}(\theta,\phi))^T \times\mathbf{G}_{\text{resp}}^{-1}(\overrightarrow{\text{resp}}-\widehat{\mathbf{SRF}}(\theta,\phi))\right), \quad (2)$$

where $\mathbf{G}_{\text{resp}}^{-1}$ denotes the covariance matrix inverse, $|\mathbf{G}_{\text{resp}}|$ is the determinant of $\mathbf{G}_{\text{resp}}$, and $\widehat{\mathbf{SRF}}(\theta,\phi)$ is the array of modeled receptive fields. The multivariate Gaussian is a well-known probability distribution (Freund, 1992), and we have previously shown that the Gaussian assumption is reasonable for first-spike latency auditory spatial receptive fields (Jenison *et al.*, 1998).

A population of 65 modeled spatial receptive fields from the left AI field in the cat was used to examine ML localization performance for a target direction (AZ 0° EL 0°) under different levels of correlated noise. The method of ML estimation entails choosing estimates of $\theta$ and $\phi$ that maximize the conditional probability or likelihood function described by Eq. (2). In this study ML estimates were obtained from the population of modeled receptive fields under a range of positive correlations between 0 and 1. Monte Carlo response simulations were performed by selecting multivariate random deviates generated by the probability model of Eq. (2), and computing the ML estimate of direction. Each experiment (simulation) entailed 300 random selections from the theoretical probability distribution. Spatial receptive fields $\widehat{\mathbf{SRF}}(\theta,\phi)$ were modeled using a spherical approximation technique described in Jenison *et al.* (1998), and an example receptive field is shown in Fig. 1(A). All neurons in the population were equally ''tuned'' using a linear combination of two radially symmetric von Mises basis functions. The width of the spatial receptive field was constructed to be approximately 60° halfway between the maximum and minimum response latencies, which is typical of contralateral virtual space receptive fields (Jenison *et al.*, 1998). The degree to which receptive fields overlap is illustrated in Fig. 1(B). The standard deviation $\sigma_i$ of the noise about the $i$th modeled receptive field was chosen to be a value of 4 ms for purposes of this paper. This is a very conservative value and represents the upper tail region of the distribution of latency standard deviations (Jenison *et al.*, 1998). The assumption of homogeneity of correlated noise is certainly not a necessary condition for computing CRLBs, however, this assumption does afford a more tractable algebraic expansion, and it may be a reasonable assumption across isofrequency bands in AI auditory cortex (Eggermont, 1992).

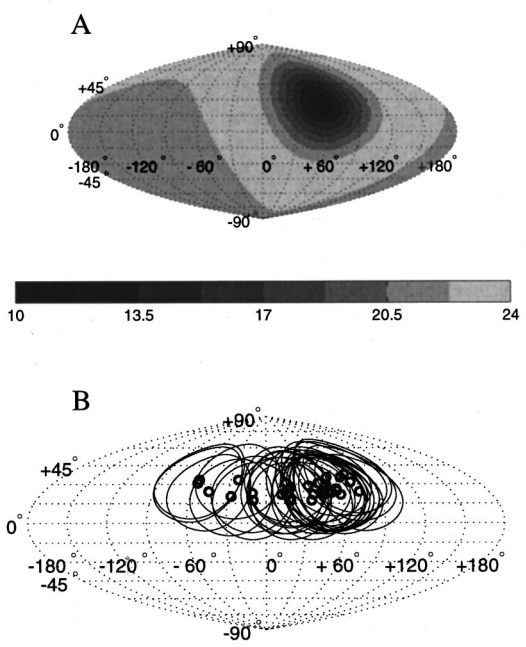


FIG. 1. (A) Example of a modeled AI cortical $\widehat{\mathbf{SRF}}$ (first-spike latency) with best direction (shortest latency at AZ 57° EL 25°). The $\widehat{\mathbf{SRF}}$ is modeled using a linear combination of spherical von Mises basis functions (Jenison *et al.*, 1998) and shown projected onto an equal-area map of auditory space. (B) A representative distribution of best directions for 65 AI $\widehat{\mathbf{SRF}}$s (circles) (from Brugge *et al.*, 1996) surrounded by iso-latency contours 50% up from the minimum latency.

## II. RESULTS

### A. Monte Carlo confirmation of theoretical lower bounds

The scatter of 300 estimates for each of the three conditions of neural response correlation is shown in Fig. 2. It is evident that the variability of the estimates generally decreases as the correlation of the response noise $\rho_{\text{resp}}$ in-

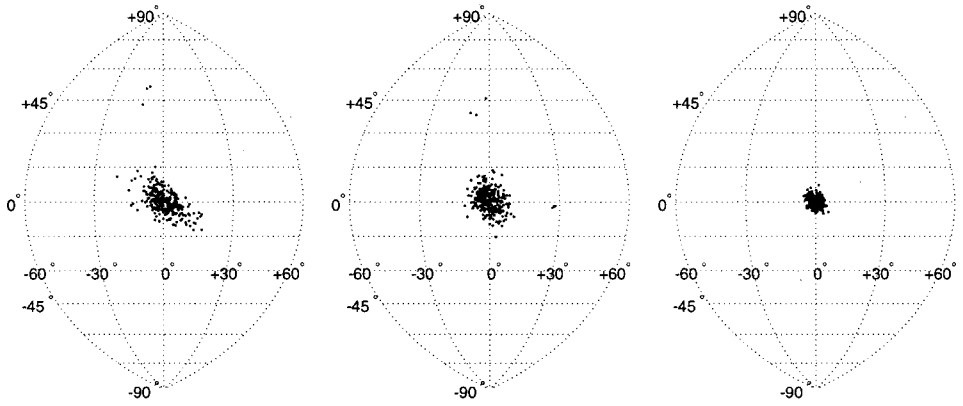


FIG. 2. Monte Carlo simulations of maximum-likelihood estimates for three levels of response correlation, $\rho_{\text{resp}}$. Each dot represents a localization estimate of a target sound source located at AZ 0° EL 0°.

creases. To reveal this trend in greater detail, 20 Monte Carlo experiments (300 estimates each) were statistically summarized as a function of $\rho_{\text{resp}}$ and are shown in Fig. 3 as circles. Plotted on top of the Monte Carlo statistics are the theoretical CRLBs. The CRLB represents a theoretical lower bound for the covariance matrix of parameter estimates, where the variance of the estimates is defined as

$$\sigma_{\hat{\theta}}^2 = E[(\hat{\theta} - E[\hat{\theta}])^2] \tag{3}$$

and

$$\sigma_{\hat{\phi}}^2 = E[(\hat{\phi} - E[\hat{\phi}])^2]. \tag{4}$$

The covariance of the estimates, $\hat{\theta}$ and $\hat{\phi}$, are defined as the product $(\rho_{\hat{\theta},\hat{\phi}})(\sigma_{\hat{\theta}})(\sigma_{\hat{\phi}})$, where $\rho_{\hat{\theta},\hat{\phi}}$ is the correlation coefficient of the estimates. The difference in definition of $\rho_{\text{resp}}$ and $\rho_{\hat{\theta},\hat{\phi}}$ may introduce some confusion at this point. $\rho_{\text{resp}}$ is the degree to which the neural noise is correlated between neurons, whereas $\rho_{\hat{\theta},\hat{\phi}}$ is the correlation between azimuth and elevation parameter estimates of sound direction generated by the theoretical ideal observer/estimator. Although $\rho_{\hat{\theta},\hat{\phi}}$ is theoretical, it is revealed empirically as the degree of corr observed in the scatter of Monte Carlo ML estimates as evident in Fig. 2. The CRLB and elements of the Fisher information matrix provide analytic insights into how correlation impacts the ML estimates. The CRLB of the estimation covariance matrix is formally defined as the matrix inverse of the Fisher information matrix (Blahut, 1987; Cover and Thomas, 1991),

$$\begin{bmatrix} \sigma_{\hat{\theta}}^2 & \rho_{\hat{\theta},\hat{\phi}}\sigma_{\hat{\theta}}\sigma_{\hat{\phi}} \\ \rho_{\hat{\theta},\hat{\phi}}\sigma_{\hat{\theta}}\sigma_{\hat{\phi}} & \sigma_{\hat{\phi}}^2 \end{bmatrix} \geqslant \mathbf{J}_{\theta,\phi}^{-1}, \tag{5}$$

where the Fisher information matrix is defined as

$$\mathbf{J}_{\theta,\phi} = \begin{bmatrix} E\left\{\frac{\partial}{\partial\theta}\log p(\overrightarrow{\text{resp}}\,|\,\theta,\phi)\right\}^2 & E\left\{\frac{\partial}{\partial\theta}\log p(\overrightarrow{\text{resp}}\,|\,\theta,\phi)\,\frac{\partial}{\partial\phi}\log p(\overrightarrow{\text{resp}}\,|\,\theta,\phi)\right\} \\ E\left\{\frac{\partial}{\partial\phi}\log p(\overrightarrow{\text{resp}}\,|\,\theta,\phi)\,\frac{\partial}{\partial\theta}\log p(\overrightarrow{\text{resp}}\,|\,\theta,\phi)\right\} & E\left\{\frac{\partial}{\partial\theta}\log p(\overrightarrow{\text{resp}}\,|\,\theta,\phi)\right\}^2 \end{bmatrix}. \tag{6}$$

Equation (5) in words states that regardless of the form of the estimator, estimation variance can never be any *smaller* than the CRLB (denoted by the inequality). The diagonal of the Fisher information matrix [Eq. (6)] corresponds to information with respect to each parameter, and the off-diagonals correspond to coupled information between parameters. Note that elements of the matrix have very subtle differences that depend on the differential operator with respect to each of the parameters, $\theta$ and $\phi$. Evaluating the expected value in the formula for Fisher information (see the Appendix) yields a computational formula for each cell in the Fisher information matrix

$$\mathbf{J}_{\theta,\phi} = \begin{bmatrix} \left\{\left[\frac{\partial}{\partial\theta}\widehat{\mathbf{SRF}}(\theta,\phi)\right]^T \mathbf{G}_{\text{resp}}^{-1}\,\frac{\partial}{\partial\theta}\widehat{\mathbf{SRF}}(\theta,\phi)\right\} & \left\{\left[\frac{\partial}{\partial\theta}\widehat{\mathbf{SRF}}(\theta,\phi)\right]^T \mathbf{G}_{\text{resp}}^{-1}\,\frac{\partial}{\partial\phi}\widehat{\mathbf{SRF}}(\theta,\phi)\right\} \\ \left\{\left[\frac{\partial}{\partial\phi}\widehat{\mathbf{SRF}}(\theta,\phi)\right]^T \mathbf{G}_{\text{resp}}^{-1}\,\frac{\partial}{\partial\theta}\widehat{\mathbf{SRF}}(\theta,\phi)\right\} & \left\{\left[\frac{\partial}{\partial\phi}\widehat{\mathbf{SRF}}(\theta,\phi)\right]^T \mathbf{G}_{\text{resp}}^{-1}\,\frac{\partial}{\partial\phi}\widehat{\mathbf{SRF}}(\theta,\phi)\right\} \end{bmatrix}. \tag{7}$$

Equation (7) illustrates the general dependence of Fisher information on the gradients of the modeled receptive fields, $(\partial/\partial\theta)\widehat{\mathbf{SRF}}(\theta,\phi)$ and $(\partial/\partial\phi)\widehat{\mathbf{SRF}}(\theta,\phi)$, and the variability of responses about the modeled receptive fields represented by the matrix $\mathbf{G}_{\text{resp}}$. Recall that $\rho_{\text{resp}}$ appears in the off-diagonal cells of $\mathbf{G}_{\text{resp}}$ [see Eq. (1)].

Figure 3 confirms that the variance of the ML estimates approaches the CRLB over many trials, as stated previously

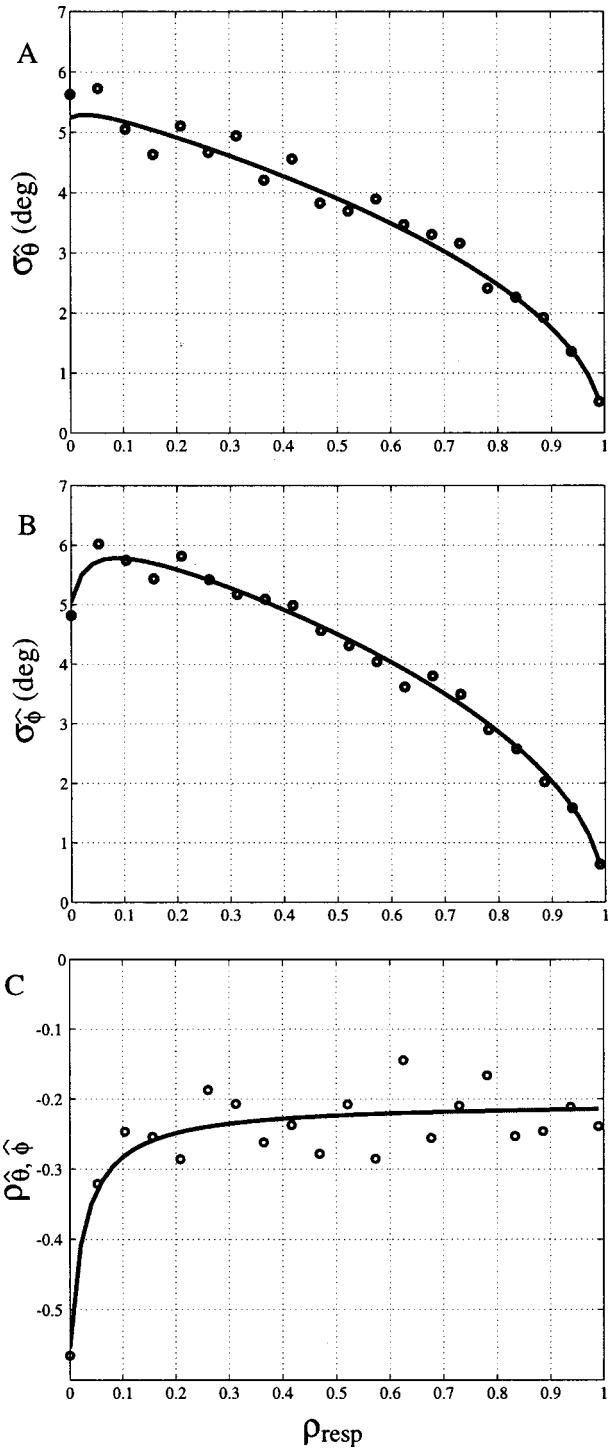


FIG. 3. Cramer–Rao Lower Bound covariance matrix [converted to (A) azimuth and (B) elevation standard deviation of the estimates, $\sigma_{\hat{\theta}}$ and $\sigma_{\hat{\phi}}$, and (C) correlation coefficients between the estimates, $\rho_{\hat{\theta},\hat{\phi}}$] (lines) for the target (true) location (AZ 0° EL 0°) as a function of response correlation, $\rho_{\text{resp}}$. Corresponding Monte Carlo statistics (circles) computed on empirical estimates as a function of response correlation, $\rho_{\text{resp}}$.

in the Introduction. It should be emphasized that each CRLB function is computed directly from the characteristics of the modeled population, and is not simply a ''fitted function'' of the Monte Carlo ML estimates. Both the Monte Carlo ML estimates and the CRLB demonstrate the trend of reduced variability of the estimates as $\rho_{\text{resp}}$ increases. Another trend that is revealed by these analyses is an asymptotic approach to a constant value of $\rho_{\hat{\theta},\hat{\phi}}$.

The shape of the CRLB functions is dependent on the position of the target (true) sound direction relative to the best directions of the population of simulated neurons. It is difficult to make general statements regarding the behavior of specific CRLB functions because they are dependent on many factors such as the slope of the receptive fields and degree of receptive field overlap. Several example sound targets are shown in Fig. 4. Since the theoretical CRLB reliably predicts the behavior of the ML estimates in the limit, only the CRLB functions of $\rho_{\text{resp}}$ are shown. Again two general trends—a reduction in variability of the estimates and the asymptotic approach to a constant value of $\rho_{\hat{\theta},\hat{\phi}}$—are evident for different target directions. The specific characteristics of the CRLB are different depending on where the target is located relative to the best directions of the cortical population. Variability of the estimates generally increases as the target moves lateral to the cluster of best directions. The magnitude and sign of the asymptotic values of $\rho_{\hat{\theta},\hat{\phi}}$ also depend on where the target is located relative to the cluster of best directions. To lend further explanation to these differences, elements of the Fisher information matrix were examined under an algebraic expansion.

### B. Analytical examination

Taylor series expansion of each cell in the Fisher information matrix helps to reveal the impact of correlation on estimation performance (acuity). The diagonal cells of the Fisher information matrix [Eq. (7)] were Taylor series expanded with respect to $\rho_{\text{resp}}$ for a population of $N$ neurons.[4] Below is shown the second-order expansion for azimuth ($\theta$) information, located in cell [1, 1] of Eq. (7):

$$J_{\theta,\phi}[1,1] \approx \sum_{i=1}^{N} \left\{ \frac{\frac{\partial}{\partial\theta}\widehat{SRF}_i(\theta,\phi)}{\sigma_i} \right\}^2 + (\mathbf{N}-1)\rho_{\text{resp}}^2 \sum_{i=1}^{N} \left\{ \frac{\frac{\partial}{\partial\theta}\widehat{SRF}_i(\theta,\phi)}{\sigma_i} \right\}^2 + ((\mathbf{N}-2)\rho_{\text{resp}}^2 - \rho_{\text{resp}}) \times \sum_{i\neq j}^{N} \left\{ \frac{\frac{\partial}{\partial\theta}\widehat{SRF}_i(\theta,\phi)\frac{\partial}{\partial\theta}\widehat{SRF}_j(\theta,\phi)}{\sigma_i\sigma_j} \right\}. \tag{8}$$

The impact of $\rho_{\text{resp}}$ can now be examined more easily because the higher-order terms of the resulting series polynomial, which have progressively less influence on the infinite series, have been removed. The removal of the higher-order terms is appropriate because higher powers of $\rho_{\text{resp}}$ must necessarily diminish because $|\rho_{\text{resp}}|<1$, which is also a necessary condition for the convergence of the series.[5] Abbott and Dayan (1999) employed a similar approach to understanding the impact of correlation, however, they focused on whether a ceiling on acuity exists as the population size approaches infinity. Here, the Taylor expansion is not restricted to large

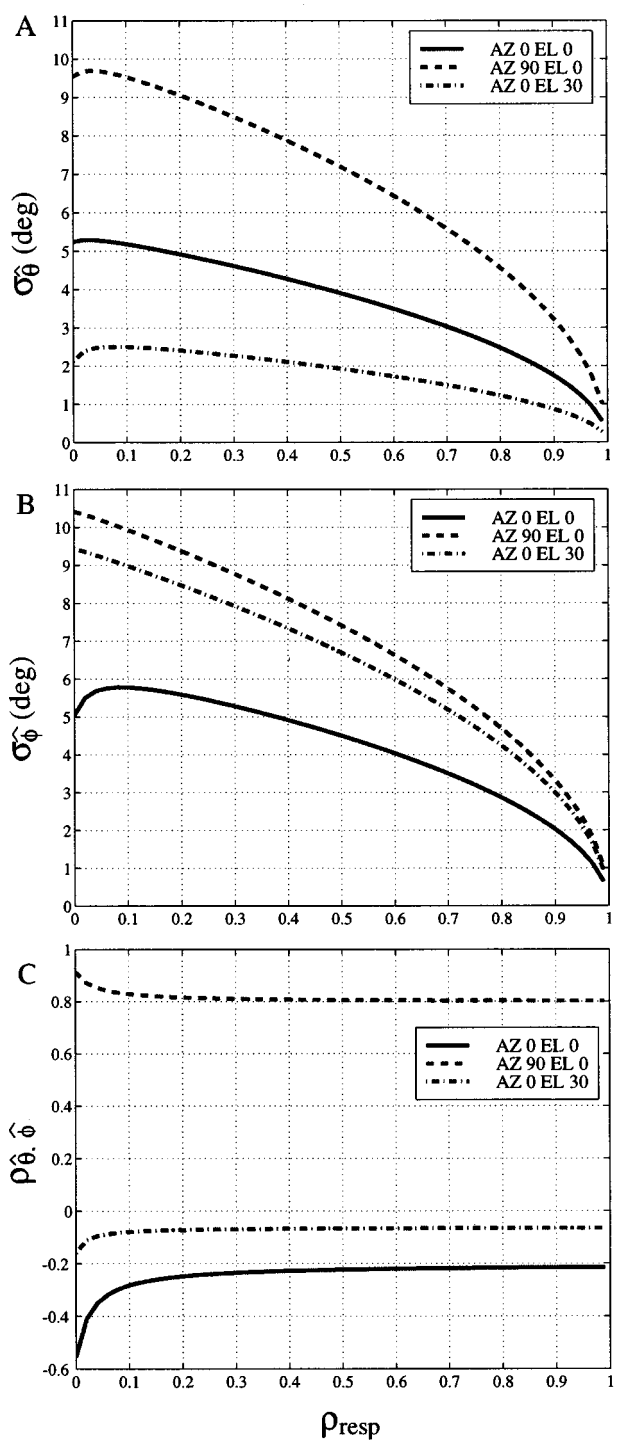


FIG. 4. Cramer–Rao Lower Bound covariance matrix [converted to (A) azimuth and (B) elevation standard deviations, $\sigma_{\hat{\theta}}$ and $\sigma_{\hat{\phi}}$, respectively, and (C) correlation coefficients between the estimates, $\rho_{\hat{\theta},\hat{\phi}}$] for three target (true) locations as a function of response correlation, $\rho_{resp}$.

*N* but considers the case of small populations. Several important influences on the magnitude of Fisher information can be observed. The first term does not depend on $\rho_{resp}$, and corresponds to the sum-of-squared $\widehat{\mathbf{SRF}}$ gradients that elevate Fisher information as *N* grows and gradients steepen, thus decreasing the lower bound on the variability of estimates. However, increasing levels of noise ($\sigma$) deflate Fisher information. Both of these observations were noted earlier by Paradiso (1988) under conditions of independence ($\rho_{resp}=0$). The second term, which *is* $\rho_{resp}$ dependent, will elevate the first term by an additional gain of $(\mathbf{N}-1)\rho_{resp}^2$. However, the story becomes more complex upon examination of the third term, where the consequence of positive correlation also depends on the direction of the receptive field gradients at a particular sound direction ($\theta$, $\phi$). Under the condition where the sum-of-products of gradients is negative, positive correlation will further elevate Fisher information with respect to the first two terms only when the corresponding gain $((\mathbf{N}-2)\rho_{resp}^2-\rho_{resp})$ has a negative sign. A negative gain necessarily occurs when $\rho_{resp}$ approaches zero and the population is small. Conversely, when the gradients possess the same sign, the third term will tend to lower Fisher information until $\rho_{resp}$ increases to a sufficiently large value. Hence, the third term in Eq. (8) provides analytical insight into the nonmonotonic behavior of the theoretical CRLBs at low values of $\rho_{resp}$ observed in Figs. 3 and 4. To survey the gain surfaces, iso-gain contours for the second and third terms are shown in Fig. 5(A) and (B), respectively. The negative region of the surface, shown in gray in Fig. 5(B), is actually concave upward with the edges corresponding to zero. It should be noted that the gain represents multiplicative factors applied to sums-of-squares and -products of gradients, and as such are isolated from the population specific characteristics (gradients and noise levels) of the receptive fields. This separation also serves to highlight the difference between systematic changes in $\widehat{\mathbf{SRF}}(\theta,\phi)$ and unsystematic covariation of the noise, which is characterized by $\rho_{resp}$. Hypothetically, two neurons with similar, but slightly different best-directions would have similar noise covariation, $\rho_{resp}$. However, depending on the direction of a sound source, the sum-of-products of gradients could be negative (when the target is between the two best-directions) or positive (when the target is lateral to the two best-directions).

### C. Violation of independence assumption

The previous analysis was based on the use of an ideal observer/estimator that has knowledge of the response covariance structure. When the response variability is correlated, the derived estimator is assumed to take advantage of this knowledge. However, the case most similar to that described by Shadlen and colleagues is when the observer is not ideal, and fails to exploit correlated variability. To contrast the nonideal case with the ideal ML estimator, Monte Carlo estimates were again obtained for the condition where the observer incorrectly assumes response independence, while response correlation is titrated into the population of responses. These results are shown in Fig. 6 under the conditions when the target was at AZ 0° EL 0° and AZ 90° EL 0°. Depending on the target direction, performance either degrades or remains relatively constant as $\rho_{resp}$ increases, for both azimuth and elevation estimates. This is in contrast to the performance of the ideal ML estimator shown in Figs. 3 and 4. Finally, correlation of the estimates $\rho_{\hat{\theta},\hat{\phi}}$ fails to approach a constant level when the assumption of response independence is violated [Fig. 6(B)]. Since the observer is suboptimal, there is not a formalism, such as a misinformed CRLB

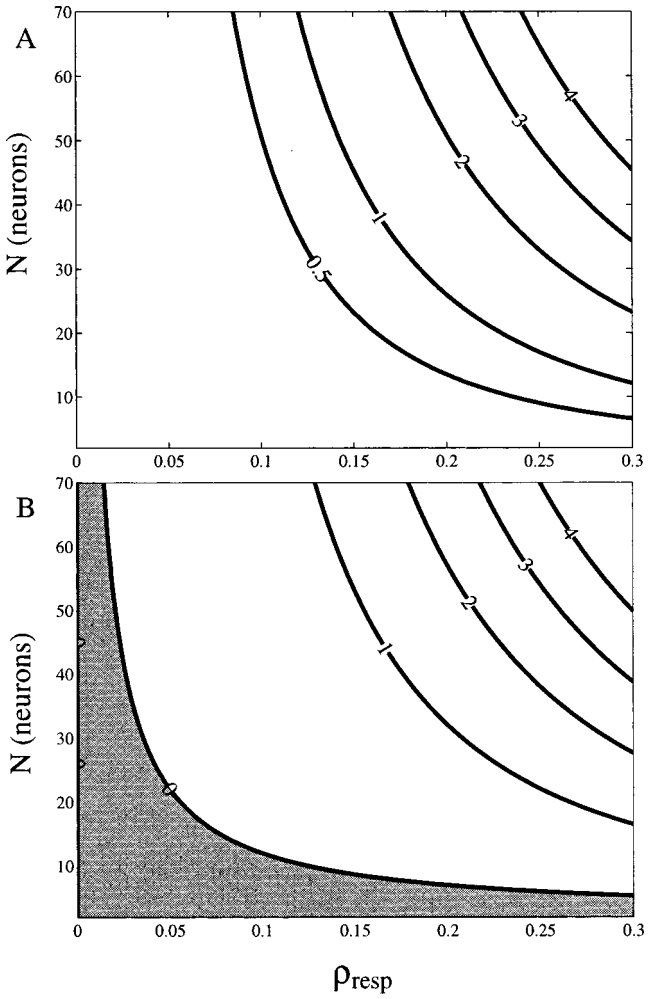


FIG. 5. Iso-gain contours for the gain functions (A) $(\mathbf{N}-1)\rho_{\text{resp}}^2$ and (B) $((\mathbf{N}-2)\rho_{\text{resp}}^2-\rho_{\text{resp}})$ of the Taylor series expanded Fisher information [Eq. (8)]. Only the lower interval of $\rho_{\text{resp}}$ is appropriate for the series expansion about the origin. Assuming $\rho_{\text{resp}}$ is nonnegative, the function in (A) is always nonnegative, and the case where the gain is negative in (B) is shown in gray.

to examine analytically. Consequently, it is difficult to interpret why estimate variability grows in certain cases, while others remain relatively constant with increasing $\rho_{\text{resp}}$. Regardless, performance does not improve with increasing $\rho_{\text{resp}}$ *under the assumption of independence*, which is a result generally consistent with earlier reports.

## III. DISCUSSION

These findings challenge the common interpretation that correlated noise between information channels always compromises ideal performance. Under the assumption of a maximum likelihood ideal observer with knowledge of the response covariance structure, the theoretical lower bounds on estimation variance generally decrease as correlation is titrated into a population of cortical neurons; we will assume that the covariance structure can be learned by the observer. Recently, this finding, while surprising, has been noted independently by several laboratories that study visual cortex (Dan *et al.*, 1998; Oram *et al.*, 1998; Abbott and Dayan, 1999). Prior to these studies, Snippe and Koenderink (1992) examined the effects of correlated noise in channel-coded

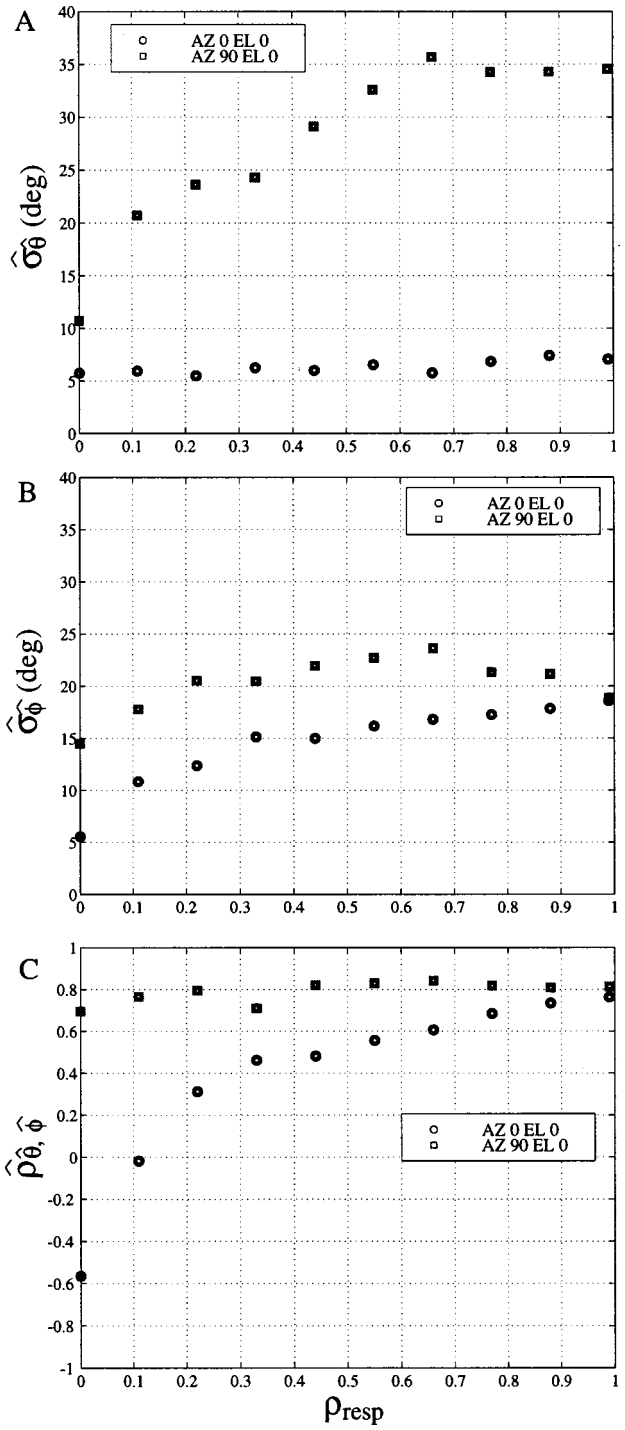


FIG. 6. Monte Carlo statistics for (A) azimuth and (B) elevation standard deviations. $\hat{\sigma}_{\hat{\theta}}$ and $\hat{\sigma}_{\hat{\phi}}$, and (C) correlation coefficients between the estimates, $\hat{\rho}_{\hat{\theta},\hat{\phi}}$ for two target (true) locations as a function of response correlation, $\rho_{\text{resp}}$, when the ML estimator incorrectly assumes independence.

systems on discrimination thresholds, coming to roughly similar conclusions, however, without the analytic tool of Fisher information. Although Abbott and Dayan (1999) have recently employed Fisher information, they did not consider the impact of correlation on cross-information between parameters. Estimation correlation, or the estimate association, approaches a constant value as more correlation is titrated into the population; that is, patterns of ML *estimates* of direction $(\theta, \phi)$ are remarkably robust to different levels of

response correlation. Correlation in behavioral estimates of sound direction relative to the median and horizontal planes have occasionally been observed in the cat (May and Huang,1996; Huang and May, 1996). The analyses here predict that direction estimates lateral to the acoustic axis will tend to evidence stronger correlation between the azimuth and elevation estimates than those near the acoustic axis. At the midline, correlation in the scatter of estimates may be cancelled when the convergence of the two contributing hemispheres is considered. Perhaps the greatest contribution of the CRLB to the analysis of the neural code is that it shares a common currency with psychophysical performance measures—that of estimation variance and $d'$. Therefore, the CRLB affords a bridge between physiology and psychophysics. Patterns of estimation error decoded from neural responses can be compared directly to patterns of estimation error generated by behavioral studies, which will help constrain the possible decoding mechanisms.


## ACKNOWLEDGMENTS

I would like to thank Dr. Rick Reale and Dr. John Brugge for their invaluable suggestions on a draft of the manuscript. I would also like to thank the two anonymous reviewers for their helpful comments. This research was supported, in part, by NIH Grant Nos. DC02804 and DC00116.


## APPENDIX

Derive cell [1, 1] in Eq. (6) from cell [1, 1] in Eq. (7):

$$\left[\frac{\partial}{\partial\theta}\widehat{\mathbf{SRF}}(\theta,\phi)\right]^T\mathbf{G}_{\mathbf{resp}}^{-1}\frac{\partial}{\partial\theta}\widehat{\mathbf{SRF}}(\theta,\phi) = E\left\{\frac{\partial}{\partial\theta}\log p(\overrightarrow{\text{resp}}\,|\,\theta,\phi)\right\}^2. \quad \text{(A1)}$$

The conditional probability density of the response is assumed to be a multivariate Gaussian PDF:

$$p(\overrightarrow{\text{resp}}\,|\,\theta,\phi) = \frac{1}{\sqrt{(2\pi)^N|\mathbf{G}_{\text{resp}}|}} \times\exp\left(-\tfrac{1}{2}(\overrightarrow{\text{resp}}-\widehat{\mathbf{SRF}}(\theta,\phi))^T \times\mathbf{G}_{\text{resp}}^{-1}(\overrightarrow{\text{resp}}-\widehat{\mathbf{SRF}}(\theta,\phi))\right), \quad \text{(A2)}$$

and taking the natural logarithm of $p(\overrightarrow{\text{resp}}\,|\,\theta,\phi)$ of Eq. (A1) yields

$$\log\left(p(\overrightarrow{\text{resp}}\,|\,\theta,\phi)\right) = \log\left(\frac{1}{\sqrt{(2\pi)^N|\mathbf{G}_{\text{resp}}|}}\right) - \tfrac{1}{2}(\overrightarrow{\text{resp}}-\widehat{\mathbf{SRF}}(\theta,\phi))^T\mathbf{G}_{\text{resp}}^{-1}(\overrightarrow{\text{resp}}-\widehat{\mathbf{SRF}}(\theta,\phi)). \quad \text{(A3)}$$

Taking the derivative of the log probability w.r.t. $\theta$ yields the bilinear form

$$\frac{\partial}{\partial\theta}\log(p(\overrightarrow{\text{resp}}\,|\,\theta,\phi) = \left[\frac{\partial}{\partial\theta}\widehat{\mathbf{SRF}}(\theta,\phi)\right]^T\mathbf{G}_{\text{resp}}^{-1} \times(\overrightarrow{\text{resp}}-\widehat{\mathbf{SRF}}(\theta,\phi)). \quad \text{(A4)}$$

We now square Eq. (A4) and take the expected value, letting

$$\mathbf{x} = (\overrightarrow{\text{resp}}-\widehat{\mathbf{SRF}}(\theta,\phi))$$

and

$$\mathbf{y} = \frac{\partial}{\partial\theta}\widehat{\mathbf{SRF}}(\theta,\phi),$$

$$E\left\{\frac{\partial}{\partial\theta}\log p(\overrightarrow{\text{resp}}\,|\,\theta,\phi)\right\}^2 = E\{\mathbf{y}^T\mathbf{G}_{\text{resp}}^{-1}\mathbf{x}\mathbf{x}^T\mathbf{G}_{\text{resp}}^{-1}\mathbf{y}\}. \quad \text{(A5)}$$

Rearrange the expected value operator

$$E\left\{\frac{\partial}{\partial\theta}\log p(\overrightarrow{\text{resp}}\,|\,\theta,\phi)\right\}^2 = \mathbf{y}^T\mathbf{G}_{\text{resp}}^{-1}E\{\mathbf{x}\mathbf{x}^T\}\mathbf{G}_{\text{resp}}^{-1}\mathbf{y}. \quad \text{(A6)}$$

$E\{\mathbf{x}\mathbf{x}^T\}$ is the covariance matrix $\mathbf{G}_{\text{resp}}$, so

$$E\left\{\frac{\partial}{\partial\theta}\log p(\overrightarrow{\text{resp}}\,|\,\theta,\phi)\right\}^2 = \mathbf{y}^T\mathbf{G}_{\text{resp}}^{-1}\mathbf{G}_{\text{resp}}\mathbf{G}_{\text{resp}}^{-1}\mathbf{y}, \quad \text{(A7)}$$

and $\mathbf{G}_{\text{resp}}^{-1}\mathbf{G}_{\text{resp}}$ is the identity matrix $\mathbf{I}$:

$$E\left\{\frac{\partial}{\partial\theta}\log p(\overrightarrow{\text{resp}}\,|\,\theta,\phi)\right\}^2 = \mathbf{y}^T\mathbf{I}\mathbf{G}_{\text{resp}}^{-1}\mathbf{y}. \quad \text{(A8)}$$

Substituting back for $\mathbf{x}$ and $\mathbf{y}$ yields the result

$$E\left\{\frac{\partial}{\partial\theta}\log p(\overrightarrow{\text{resp}}\,|\,\theta,\phi)\right\}^2 = \left[\frac{\partial}{\partial\theta}\widehat{\mathbf{SRF}}(\theta,\phi)\right]^T \times\mathbf{G}_{\text{resp}}^{-1}\frac{\partial}{\partial\theta}\widehat{\mathbf{SRF}}(\theta,\phi). \quad \text{(A9)}$$

The same steps can be applied to derive the remaining cells of the Fisher information matrix, under the assumption of multivariate Gaussian noise.

[1]The details of spherical functional approximation can be found in Jenison *et al.* (1998). The spatial receptive field model is expressed as:

$$\widehat{\mathbf{SRF}}(\theta,\phi) = \sum_{m=1}^{M} W_m\exp\{k_m[\sin\phi\sin\beta_m\cos(\theta-\alpha_m)+\cos\phi\cos\beta_m]\},$$

where $M$ is the number of basis functions, $\alpha_m$ and $\beta_m$ are the coordinates of the basis function centroids, $\kappa_m$ is the concentration parameter, and $w_m$ is a weight.

[2]Sometimes a source of confusion, the ''hat'' ($\hat{}$) is also used to denote a physical parameter estimate, such as $\hat{\theta}$. It is also used in connection with Monte Carlo simulations where a population parameter is being estimated from a random sample; for example, $\hat{\sigma}_{\hat{\theta}}^2$ is the Monte Carlo estimate of the theoretical $\sigma_{\hat{\theta}}^2$.

[3]The assumption of homogeneity refers only to correlation, not the covariance matrix. The standard deviations are not assumed to be homogeneous, hence the covariance matrix is not homogeneous.

[4]The Taylor series expansions differ only by the gradients $(\partial/\partial\theta)\widehat{\mathbf{SRF}}_i(\theta,\phi)$ and $(\partial/\partial\phi)\widehat{\mathbf{SRF}}_i(\theta,\phi)$. The series expansion is performed about $\rho_{\text{resp}}=0$.

[5]Sufficient conditions have also been met such that the Taylor series expansion of Eq. (7) is guaranteed to converge.

Abbott, L. F., and Dayan, P. (**1999**). ''The effect of correlated variability of a population code,'' Neural Comput. **11**, 91–94.
Blahut, R. E. (**1987**). *Principles and Practice of Information Theory* (Addison-Wesley, Reading, MA).
Brugge, J. F., Reale, R. A., and Hind, J. E. (**1996**). ''The structure of spatial receptive fields of neurons in primary auditory cortex of the cat,'' J. Neurosci. **16**, 4420–4437.
Cover, T. M., and Thomas, J. A. (**1991**). *Elements of Information Theory* (Wiley, New York).
Dan, Y., Alonso, J. M., Usrey, W. M., and Reid, R. C. (**1998**). ''Coding of visual information by precisely correlated spikes in the lateral geniculate nucleus,'' Nat. Neurosci. **1**, 501–507.
Eggermont, J. J. (**1992**). ''Neural interaction in cat primary auditory cortex. Dependence on recording depth, electrode separation, and age,'' J. Neurophysiol. **68**, 1216–1228.
Fisher, R. A. (**1925**). ''Theory of statistical estimation,'' Proc. Cambridge Philos. Soc. **22**, 700–725.
Freund, J. F. (**1992**). *Mathematical Statistics* (Prentice-Hall, Englewood Cliffs, NJ).
Huang, A. Y., and May, B. J. (**1996**). ''Sound orientation behavior in cats. II. Mid-frequency spectral cues for sound localization,'' J. Acoust. Soc. Am. **100**, 1070–1080.
Jenison, R. L. (**1998**). ''Models of sound location acuity with broad cortical spatial receptive fields,'' in *Central Auditory Processing and Neural Modeling*, edited by P. Poon and J. F. Brugge (Plenum, New York), pp. 161–174.
Jenison, R. L., Reale, R. A., Hind, J., and Brugge, J. F. (**1998**). ''Modeling auditory spatial receptive fields with spherical approximation functions,'' J. Neurophysiol. **80**, 2645–2656.
May, B. J., and Huang, A. Y. (**1996**). ''Sound orientation behavior in cats. I. Localization of broadband noise,'' J. Acoust. Soc. Am. **100**, 1059–1069.
Musicant, A. D., Chan, J. C. K., and Hind, J. E. (**1990**). ''Direction-dependent spectral properties of cat external ear: New data and cross-species comparisons,'' J. Acoust. Soc. Am. **87**, 757–781.
Oram, M. W., Foldiak, P., Perrett, D. I., and Sengpiel, F. (**1998**). ''The 'Ideal Homunculus': Decoding neural population signals,'' Trends Neurosci. **21**, 259–265.
Paradiso, M. A. (**1988**). ''A theory for the use of visual orientation information which exploits the columnar structure of striate cortex,'' Biol. Cybern. **58**, 35–49.
Pouget, A., Zhang, K., Deneve, S., and Latham, P. E. (**1998**). ''Statistically efficient estimation using population codes,'' Neural Comput. **10**, 373–401.
Seung, H. S., and Sompolinsky, H. (**1993**). ''Simple models for reading neuronal population codes,'' Proc. Natl. Acad. Sci. USA **90**, 10749–10753.
Shadlen, M. N., Britten, K. H., Newsome, W. T., and Movshon, J. A. (**1996**). ''A computational analysis of the relationship between neuronal and behavioral responses to visual motion,'' J. Neurosci. **16**, 1486–1510.
Shadlen, M. N., and Newsome, W. T. (**1998**). ''The variable discharge of cortical neurons: Implications for connectivity, computation, and information coding,'' J. Neurosci. **18**, 3870–3896.
Snippe, H. P., and Koenderink, J. J. (**1992**). ''Information in channel-coded systems: Correlated receivers,'' Biol. Cybern. **67**, 183–190.
Zohary, E., Shadlen, M. N., and Newsome, W. T. (**1994**). ''Correlated neuronal discharge rate and its implications for psychophysical performance,'' Nature (London) **370**, 140–143.